AAS 21-344

A MODIFIED ORBIT CHAINING FRAMEWORK FOR LOW-THRUST TRANSFERS BETWEEN ORBITS IN CISLUNAR SPACE

Bonnie Prado Pino*, Kathleen C. Howell† and David C. Folta‡

In an effort to explore further extended mission options for the secondary payload riding along the NASA Artemis-1 spacecraft[1], the Lunar IceCube (LIC) satellite, new interest arises into the problem of constructing a general framework for the initial guess generation of low-thrust trajectories in cislunar space, that is independent of the force models in which the orbits of interest are defined. Given the efficiency of the LIC low-thrust engine[2], after completion of its primary science and technology demonstrations in an orbit around the Moon, the spacecraft could perform further exploration of the cislunar space. In this investigation, a generalized strategy for constructing initial guesses for low-thrust spacecraft traveling between lunar orbits that exist within the context of multiple dynamical models is presented. These trajectories are converged as mass-optimal solutions in lower fidelity model, that are easily transitioned and validated in the higher fidelity ephemeris model, and, achieve large orbital plane changes while evolving entirely within the cislunar region.

INTRODUCTION

The low-thrust enabled trajectories in the Circular Restricted Three-Body Problem (CR3BP) are often referred to as low-energy transfers. These transfer have been computed by many authors using different techniques, some of which include the addition of natural or ballistic arcs in the construction of the initial estimate for the trajectory[3]. Some examples of previously flown low-thrust missions include the Deep Space 1[4] mission to the McAuliffe asteroid and the West-Kohoutek-Ikemura comet, the Dawn[5] mission to the dwarf planets Vesta and Ceres, and the Hayabusa 1 and 2[6] missions to the Itokawa and Ryugu asteroids. Moreover, some examples of future low-thrust missions include the Lunar IceCube spacecraft, and NASA's Gateway mission. As low-thrust technologies continue to be developed and tested, the number of low-thrust-enabled missions within the context of the CR3BP will increase, and more strategies will need to be designed and validated.

In the low-thrust trajectory design framework for specified departure and arrival orbits, one such approach for constructing initial guesses is that of the orbit chaining strategy, whose goal is to leverage the natural dynamics that exists within any dynamical model, to patch together intermediate arcs that reside in the vicinity of the departure and arrival orbits, aiding in the construction of an informed initial guess for the low-thrust transfer[7]. Typically, these intermediate arcs consist of either periodic orbits that exist within the context of lower fidelity force models, or, natural structures,

*PhD Candidate, School of Aeronautics and Astronautics, Purdue University, West Lafayette, IN 47906, USA; currently, Astrodynamics Engineer, LeoLabs, Inc., Menlo Park, CA. bpradopi@purdue.edu

†Hsu Lo Distinguished Professor, School of Aeronautics and Astronautics, College of Engineering, Purdue University, West Lafayette, IN 47906. howell@purdue.edu

‡NASA Goddard Space Flight Center, Greenbelt, MD 47906. david.c.folta@nasa.gov

such as manifold arcs, that traverse the region of interest in space. To select an appropriate set of intermediate arcs, previous studies have demonstrated the utilization of an energy parametrization of the space to generate fully continuos paths in position, velocity and mass states, and, to deliver mass-optimal solutions[8].

Following the work of Prado Pino, Pritchett, Howell and Folta[9], for the distinct applications of interest explored in this investigation, it is assumed that a CubeSat-type low-thrust spacecraft departs from an orbit that exists within the context of the Circular Restricted Three-Body Problem (CR3BP), and arrives at an orbit defined within the context of the Two-Body Problem (2BP) in the vicinity of the Moon. A modified approach to the orbit chaining strategy is developed to construct initial guesses for these multi-force model low-thrust transfers, that employs intermediate arcs from both dynamical models in the generation of the initial guess for the trajectory. To further validate the results, all transfers generated between multi-body orbits are transitioned into a higher fidelity ephemeris model that includes the gravitational perturbations of the Sun, the Earth and the Moon, such that, the framework developed in this investigation is valid regardless of the force model in which the departure and arrival orbits exits. A step-by-step approach for this framework is provided for the construction of informed initial guesses for the low-thrust trajectory design problem.

The methodology presented in this work leverages the intersection of combining the traditional orbit chaining framework with an energy-informed adaptive sliding algorithm, adaptable to operate under multiple force models, to construct low-thrust transfers over a range of cislunar problems of varying complexity. The geometry of all transfers explored in this investigation correspond to interior-type low-thrust trajectories, for which the spacecraft does not depart the lunar vicinity to successfully accomplish the desired plane and inclination changes; rather, the spacecraft slides through a bounded region of space while leveraging the natural motion that exist in the vicinity, within the context of multiple dynamical models. Consequently, cislunar low-thrust trajectories exploiting the continuous evolution in amplitude and Jacobi constant values across families of multi-body periodic orbits in the vicinity of the Moon are generated, that gradually modify their energy and inclination.

The process of designing trajectories for spacecraft in cislunar orbits is similar whether the vehicle is propelled by a chemical engine or within a low-thrust regime[10]; it starts with the construction of an initial guess for the spacecraft's path. As numerical methods are iterative by nature, the algorithms are initialized with a user supplied initial condition; successive updates are made that drive the initial estimate to meet all the problem constraints until a converged solution is found. The initial guess of the trajectory not only drives the geometry of the converged path, but also determines the successful performance of the algorithm, as poor initial guesses might cause a corrections process or an optimizer to diverge. The construction of an informed initial guess for a numerical method is then a important area of research that is currently still under development.

The low-thrust trajectory design problem still poses challenges when analyzed as an optimal control problem, since the determination of the control variables that optimize an objective function —typically propellant consumption or time-of-flight— is a non trivial process[11]. There exist multiple techniques to address the initial guess generations of low-thrust spacecraft trajectories[12], one of which is the orbit chain approach. In this investigation, a natural parameter continuation method is successfully introduced into the implementation of a generalized modified orbit chaining technique, that leverages an energy-informed adaptive sliding algorithm to navigate the cislunar space in the creation of informed initial guesses, and delivers optimal trajectories for low-thrust spacecraft moving in the vicinity of the Moon.

DYNAMICAL MODEL: LOW-THRUST $\mathcal{N}$-BODY PROBLEM

To represent the motion of a low-thrust spacecraft, P_3, moving with respect to a primary body, P_q, in a time-dependent system, under perturbations from the gravitational influences of $\mathcal{N}$ additional nearby bodies, as represented in Figure 1, let $\tilde{T}$ represent the dimensional thrust acceleration magnitude, M correspond to the dimensional mass of the spacecraft, M_j $(j = 1, \cdots, n)$ be the dimensional mass of each additional perturbing body, and $\tilde{G}$ be the dimensional gravitational constant. The spacecraft's acceleration vector expressed in a J2000 inertial reference coordinate frame, centered on the primary body[13], is given by:

$$\ddot{\bar{R}}_{q3} = -\frac{\tilde{G}M_q}{R_{q3}^3}\bar{R}_{q3}^3 + \tilde{G}\sum_{j=1, j\neq q,3}^{\mathcal{N}} M_j\left(\frac{\bar{R}_{3j}}{R_{3j}^3} - \frac{\bar{R}_{qj}}{R_{qj}^3}\right) + \frac{\tilde{T}}{M}\hat{a}_T \tag{1}$$

where the unit vector $\hat{a}_T$ represents the thrust orientation vector, the vector $\bar{R}_{q3}$ corresponds to the inertial dimensional position vector from the primary body to the spacecraft, the vector $\bar{R}_{qj}$ is the dimensional position vector from each perturbing body to the primary body in inertial coordinates, and the vector $\bar{R}_{3j}$ corresponds to the dimensional inertial position vector from the spacecraft to each of the perturbing bodies.

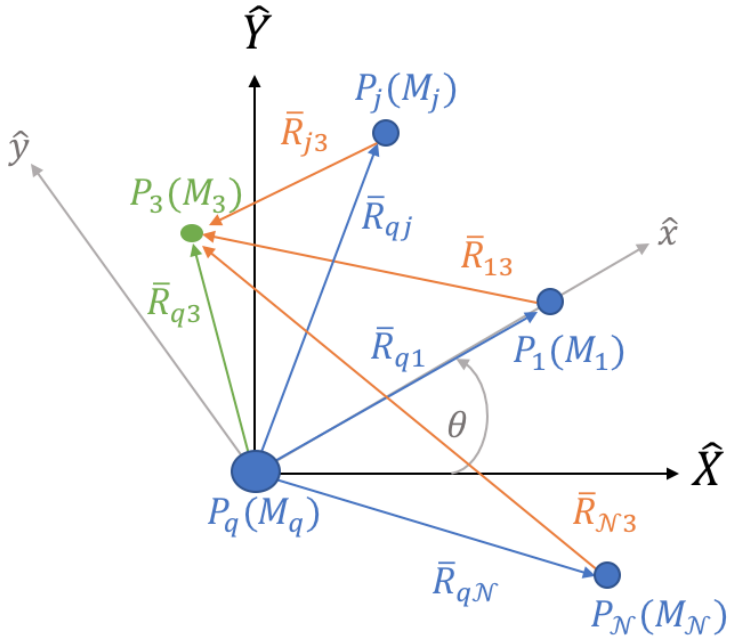

Figure 1. Graphical representation of the $\mathcal{N}-$body problem. Particle P_j under the gravitational influence of $\mathcal{N}-1$ attracting bodies

Equation 1 is derived in dimensional inertial coordinates following a Newtonian approach, as follows: the inertial position vector from the central body, P_q, to the spacecraft, P_3, is given by:

$$\bar{R}_{q3} = \bar{R}_3 - \bar{R}_q \tag{2}$$

Since these position vectors are all expressed in terms of inertial cartesian components, the time derivative with respect to an inertial frame are straightforward —there is no need to utilized the basic kinematic equation— hence, the inertial position and velocity of the spacecraft with respect to the central body are:

$$
\begin{aligned}
{}^{\mathbf{I}}\dot{\bar{R}}_{q3} &= {}^{\mathbf{I}}\dot{\bar{R}}_3 - {}^{\mathbf{I}}\dot{\bar{R}}_q && (3)\\
{}^{\mathbf{I}}\ddot{\bar{R}}_{q3} &= {}^{\mathbf{I}}\ddot{\bar{R}}_3 - {}^{\mathbf{I}}\ddot{\bar{R}}_q && (4)
\end{aligned}
$$

Applying Newton's second law of gravity, the individual inertial acceleration terms in Equations 3 and 4 are expressed as:

$$
\begin{aligned}
M_q {}^{\mathbf{I}}\ddot{\bar{R}}_q &= -\tilde{G}\sum_{j=1,j\neq q}^{\mathcal{N}} \frac{M_q M_j}{R_{jq}^3}\bar{R}_{jq} && (5)\\
M_3 {}^{\mathbf{I}}\ddot{\bar{R}}_3 &= -\tilde{G}\sum_{j=1,j\neq 3}^{\mathcal{N}} \frac{M_3 M_j}{R_{j3}^3}\bar{R}_{j3} && (6)
\end{aligned}
$$

Substituting Equations 5 and 6 into Equation 4, yields:

$$
{}^{\mathbf{I}}\ddot{\bar{R}}_{q3} = -\frac{\tilde{G}}{M_3}\sum_{j=1,j\neq q}^{\mathcal{N}} \frac{M_3 M_j}{R_{jq}^3}\bar{R}_{jq} + \frac{\tilde{G}}{M_3}\sum_{j=1,j\neq 3}^{\mathcal{N}} \frac{M_3 M_j}{R_{j3}^3}\bar{R}_{j3} \tag{7}
$$

Simplifying the mass of the spacecraft, M_3, from the above equation, and reversing the orientation of the inertial position vectors of the spacecraft with respect to the primary —perturbing— bodies yields:

$$
{}^{\mathbf{I}}\ddot{\bar{R}}_{q3} = \tilde{G}\sum_{j=1,j\neq 3}^{\mathcal{N}} \frac{M_j}{R_{3j}^3}\bar{R}_{3j} - \tilde{G}\sum_{j=1,j\neq q}^{\mathcal{N}} \frac{M_j}{R_{qj}^3}\bar{R}_{qj} \tag{8}
$$

Finally, to arrive at Equation 1, isolate the $j = 3$ term from the second term in Equation 8, and combine the two summations into one.

The acceleration term introduced by the low-thrust engine to the equations of motion, is valid independently of the engine model assumed, i.e., it is valid for both the Constant Specific Impulse (CSI) engine model, as well as the Variable Specific Impulse (VSI) regime[14]. Furthermore, the relationship between the engine specific impulse, I_{sp}, and the magnitude of the thrust force is given by:

$$
\tilde{T} = \frac{2\mathcal{P}}{I_{sp} g_0} \tag{9}
$$

where g_0 is the dimensional reference gravitational acceleration constant for the system of interest. Furthermore, in a CSI regime, in which the power of the engine is assumed to be constant, the

control authority on the trust acceleration magnitude is restricted to a turn-and-hold type of regime, such that:

$$\tilde{T} = \begin{cases} \text{engine on, } \tilde{T} = \tilde{T}_{max} \\ \text{engine off, } \tilde{T} = 0 \end{cases}$$

and, the mass flow rate of the spacecraft is computed analytically as:

$$\dot{m} = -\frac{\tilde{T}}{I_{sp} g_0} \tag{10}$$

note that, the equation for the mass rate of flow under the CSI regime possesses an analytical solution, whereas, in a VSI regime, the mass flow rate of the spacecraft must be integrated as part of the state vector to obtain its time history.

Lastly, recall that the J2000 coordinate frame is an Earth-centered inertial reference frame where all directions are recorded on January 1st, 2000 at 12:00:00 Ephemeris Time (ET) (Julian Date: 2451545.0 ET), in which the *x*-axis is directed along the vernal equinox, the z-axis is parallel to the Earth spin axis direction, and the *y*-axis completes the right-handed triad. The relative position quantities in Equation 1 associated with the gravitational bodies, are accessed via SPICE toolkits, and are computed from the NASA's Jet Propulsion Laboratory DE421 ephemerides data[15].

In this investigation, the solutions computed in the J2000 inertial reference frame are transformed into alternate frames inertial and rotating in the ephemeris models for further analysis. For instance employing the Moon as the central body in the inertial frame is of great advantage when visualizing trajectories between libration point orbits in the cislunar region. There exist multiple approaches for transforming trajectories from a primary body centered inertial frame to a barycentered rotating frame[16].

TRADITIONAL ORBIT CHAINING FRAMEWORK

The traditional orbit chaining framework utilizes natural arcs —or any other dynamical structure— within the context any any force model to employ as intermediate segments in the construction of robust initial guesses for the trajectory design problem[17]. When combining the traditional orbit chaining scheme with an energy-informed adaptive sliding algorithm, this framework is able to identify the minimum number of intermediate arcs required to traverse the gaps in position and velocity space between a departure and an arrival orbit.

To estimate the minimum number of intermediate arcs, or minimum number of segments in a chain, a parametrization of the energy evolution for families of orbits that exists in the vicinity of the region of interest, along with the accessible region —in configuration space— provided by the thrust capabilities of the spacecraft is utilized and the trajectory is converged by minimizing the following objective function:

$$J = \min_{N \in \mathbb{N}} \left\{ \left(\frac{1}{2} \sum_{j=1}^{N} \Delta C_j^2 \right) \right\} \tag{11}$$

where ΔC_j represents the change in energy for each intermediate orbit as reflected in the corresponding value of the Jacobi constant, and N is the number of intermediate orbits utilized. Furthermore, if it is desired to generate orbits that do not depart the vicinity of interest, the traditional orbit chaining approach is formulated by following the six-steps below:

1. Analyze any dynamical structures that exist in the vicinity of the departure and arrival orbits, regardless of the force model in which those orbits exist
2. Select natural arcs that offer high-efficiency energy paths, independent of the time-of-flight
3. Clip the sections of the arcs that best suit the transfer requirements and form an initial guess
4. Subdivide the initial guess for the trajectory into smaller segments and patch points, such that those can be incorporated in a differential corrections process
5. If needed, stack additional revolutions of the initial and final orbits as appropriate
6. For the low-thrust trajectory design problem, define the control history of the thrust acceleration vector by utilizing either a differential corrections process or an optimizer, to produce a converged solution

The algorithm described in the steps above, delivers the initial guess for the trajectory design problem based solely on an energy parametrization of the space, for which the following relationship is assumed:

$$\Delta C = C_{departure} - C_{arrival} = C_i - C_f$$

where $C_{departure} = C_i$ represents the energy of the initial —departure— orbit, and $C_{arrival} = C_f$ corresponds to the energy of the final —destination— orbit. Moreover, since a predetermined number of intermediate orbits is sought, the energy relationship can also be written in terms of the change in energy between each pair of intermediate orbits as follows:

$$C_f = C_i + \sum_{j=1}^{N} \Delta C_j \tag{12}$$

A sample illustration of the implementation of the traditional orbit chaining framework combined with the adaptive sliding algorithm is presented in Figure 2, to deliver a low-thrust spacecraft from a L_2 Lyapunov orbit in the vicinity of the Moon to a L_4 Short Period Orbit (SPO), within the context of the CR3BP. Figure 2(a) represents the initial guess generated by following the steps of the trajectory design framework; Figure 2(b) corresponds to the converged locally optimal solution delivered by the algorithm. Red and blue segments represent the arcs for which the spacecraft is thrusting and coasting, respectively.

In this application, the algorithm selects two members of the family of the departure orbits, and two members of the family of the arrival orbit as the minimum number of intermediate orbits needed to accomplish such low-thrust transfer. Furthermore, the change in energy required per intermediate orbit is a function of the thrust acceleration level, as well as the thrust propagation duration; hence, the minimum number of intermediate arcs computed by the optimization problem embedded in the traditional orbit chaining algorithm described in this section, also depends on the physical capabilities of the spacecraft.

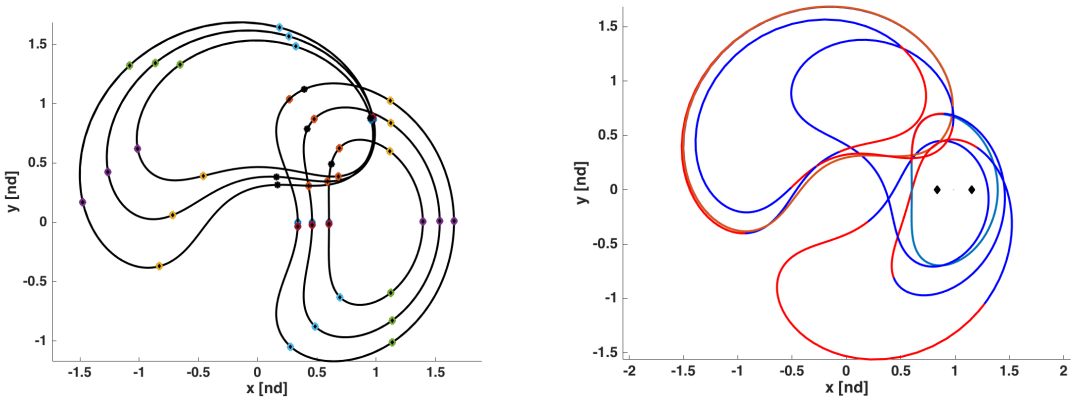

(a) Traditional Orbit Chaining - Initial Guess

(b) Traditional Orbit Chaining - Converged Transfer

Figure 2. Mass Optimal LT Transfer from a L_2 S NRHO to the First Member of the Family of Destination Orbits in the CR3BP-LT Model

MODIFIED ORBIT CHAINING FRAMEWORK

The modified orbit chaining strategy consist of dividing the problem of transferring a low-thrust spacecraft from a departure to an arrival orbit into subproblems. From the target arrival orbit, a family of destination orbits is constructed via a continuation method[18], such that, the first member of said family is the target arrival orbit, and, the last member is the last orbit computed via the continuation method. The goal of the first subproblem in the modified orbit chaining strategy delivers the spacecraft from the departure orbit to the last member of the family of arrival orbits, and each subsequent subproblem utilizes the previously generated converged solution, to deliver the spacecraft from the departure orbit to the next member of the family of destinations orbits. The problem is divided into as many subproblems as the number of destination orbits created in the family of arrival orbits.

To better illustrate the framework, consider a low-thrust CubeSat spacecraft, traveling from a Southern (N) Near Rectilinear Halo Orbit (NRHO) in the vicinity of the L_2 libration point, to a Northern (N) elliptical Low Lunar Orbit (LLO) with a perilune and apolune altitude of 100 km and 5,000 km, respectively. To divide the problem into subproblems, a family of destination orbits is generated; the first member of the family is the target arrival elliptical lunar orbit; the last member of the family is an L_2 N NRHO with a 100 km perilune altitude. Note that, these two orbits —the LLO and the NRHO— exist within the context of two different force model, thus, a creative approach must be utilized to overcome the differences in the dynamical models.

The goal of the first subproblem is to transfer the spacecraft from the departure southern NRHO to the northern 100 km perilune altitude NRHO. Once this solution is identified and fully converged utilizing a differential corrections scheme, a path for the spacecraft to move from the southern into the northern hemisphere of the z-plane is established. The goal of each subsequent subproblem is to construct fully continuous solutions to each of the next destination orbits in the family of arrival orbits, always utilizing the previously converged solution as the initial guess for the next subproblem, until the spacecraft is successfully delivered from the departure orbit to the target arrival LLO. This process is described in the following steps:

1. Propagate the departure L_2 S NRHO orbit in the CR3BP dynamical model
2. Define the arrival elliptical orbit in the 2BP force model. An example of such Keplerian orbit appears in Figure 3, represented in inertial coordinates centered at the Moon. This orbit exerts a perilune and apolune altitude of 100km and 5,000km, respectively

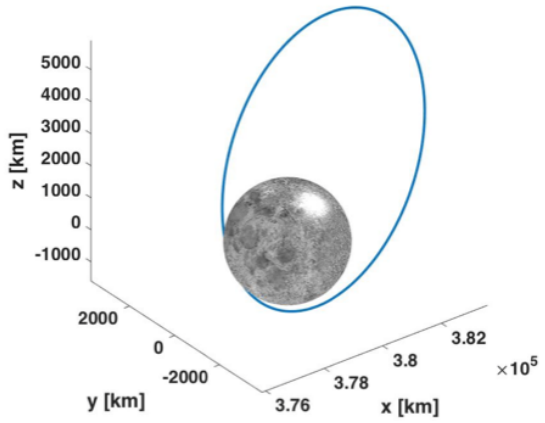

Figure 3. Elliptical Northern Low Lunar Orbit in the 2BP model. 100 km Perilune Altitude; 5,000 km Apolune Altitude

3. Perform a natural parameter continuation method on the target arrival LLO from Step 2 by systematically increasing the altitude of the apoapsis of the elliptical orbit, while keeping the perilune altitude fixed. A family of multiple destination orbits, that share the same periapsis altitude, is achieved as appears in Figure 4. Each colored orbit represents a different member of the family of 100 km-perilune altitude northern elliptical lunar orbits, represented in inertial 2BP coordinates centered at the Moon

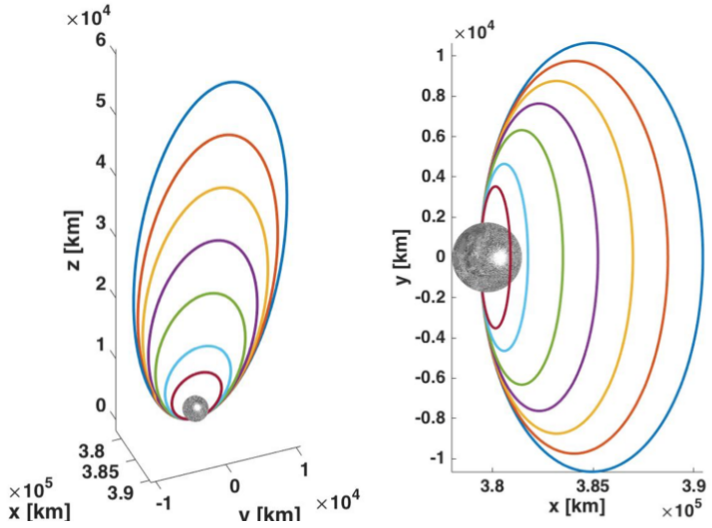

(a) 3D View of Family of Northern LLOs in the 2BP model

(b) Planar Projection of Family of Northern LLOs in the 2BP model

Figure 4. Family of Northern Elliptical LLOs in the 2BP Model

4. For each elliptical orbit in Step 3, transform the position and velocity states from the 2BP to CR3BP coordinates centered at the Earth-Moon barycenter. A three-dimensional view and a planar projection of this family of elliptical lunar orbits, within the context of the CR3BP force model is depicted in Figure 5, along with the departure southern NRHO orbit shown in black

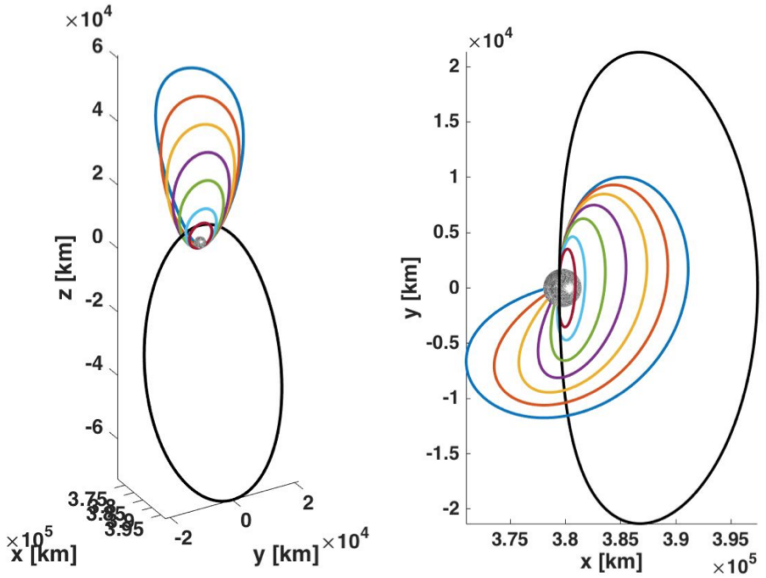

(a) 3D View of Family of Northern LLOs in the CR3BP model

(b) Planar Projection of Family of Northern LLOs in the CR3BP model

Figure 5. Family of Northern Elliptical LLOs in the CR3BP Model

5. First subproblem: Let the last member of the family of arrival orbits be a L_2 N NRHO with a 100 km perilune altitude and 65,581.3 km apolune altitude. The goal of this subproblem is to generate a fully converged solution from the departure orbit to the L_2 N NRHO. Utilizing manifold arcs from the departure and arrival orbits, construct the initial guess shown in Figure 6(a) and converge it into a continuous path as it appears in Figure 6(b)

6. Second subproblem: Utilize the converge solution generated in Step 5 as the initial guess for the second subproblem, whose goal is to deliver the spacecraft from the departure L_2 S NRHO to the next member of the family of arrival orbits created in Step 3. The new destination orbit is now a northern elliptical lunar orbit with a 100 km perilune altitude, and an apoapsis altitude closer to the apoapsis of the L_2 N NRHO from Step 5, 60,000 km, that has been transformed from the 2BP to the CR3BP dynamical model. The converged solution for the second subproblem is depicted in Figure 7

7. Repeat Step 6 for each subsequent orbit in the family of 100 km perilune altitude destination elliptical lunar orbits until arrival on the original target LLO

The modified orbit chaining framework proposed in this investigation, utilizes the traditional orbit chaining approach combined with an energy-informed adaptive sliding algorithm scheme to solve

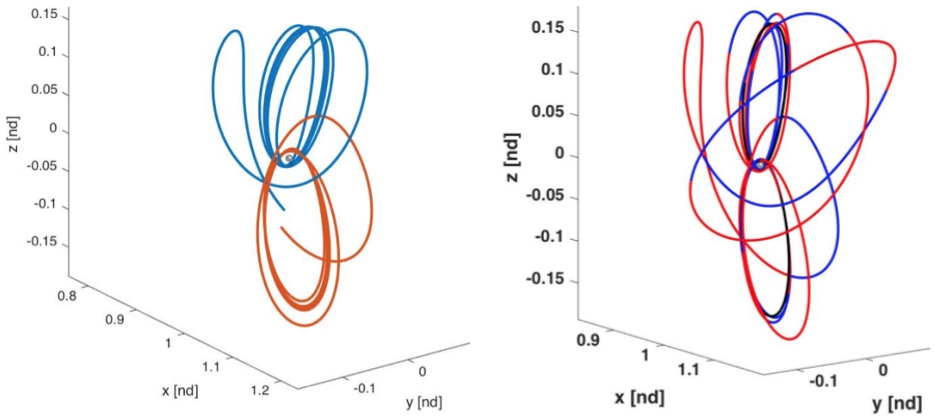

(a) Initial Guess for a Transfer from a L_2 S NRHO to a L_2 N NRHO

(b) Converged Solution for a Transfer from a L_2 S NRHO to a L_2 N NRHO

Figure 6. Low-Thrust Transfer from a L_2 S NRHO to a L_2 N NRHO. Red and Blue Segments Correspond to Thrust and Coast Arcs, Respectively

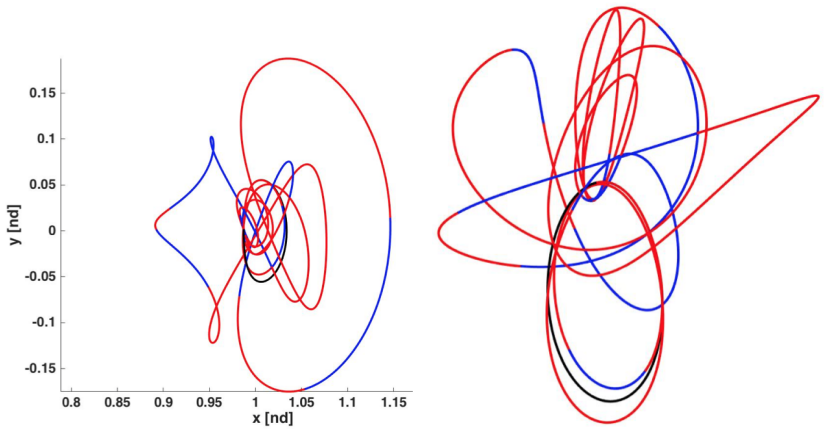

(a) Planar Projection. Low-Thrust Transfer from a L_2 S NRHO to a northern elliptical lunar orbit with 100 km perilune altitude, and 60,000 km apolune altitude

(b) 3D View. Low-Thrust Transfer from a L_2 S NRHO to a northern elliptical lunar orbit with 100 km perilune altitude, and 60,000 km apolune altitude

Figure 7. Low-Thrust Transfer from a L_2 S NRHO to a northern elliptical lunar orbit with 100 km perilune altitude, and 60,000 km apolune altitude. Red and Blue Segments Correspond to Thrust and Coast Arcs, Respectively

a subproblem that, in theory, results less computationally expensive than the original departure-destination low-thrust transfer design problem, and, by leveraging numerical continuation techniques, approaches the solution to the original problem in a smooth and convergence-guaranteed fashion.

APPLICATION: MASS-OPTIMAL TRANSFER FROM A L_2 SOUTHERN NRHO TO A CIRCULAR LOW LUNAR ORBIT

Upon deployment as a secondary payload from the Artemis-1 spacecraft, Lunar IceCube (LIC), a 6U CubeSat equipped with a 1.24mN maximum thrust engine, will transfer to an orbit in the lunar vicinity from which it will complete its primary science and technology demonstration objectives[19]. It is assumed in this investigation, that the primary science mission orbit is a member of the L_2 Southern (S) Near Rectilinear Halo Orbits (NRHO). While the efficiency of LIC's low-thrust engine enables the spacecraft to pursue extended mission objectives[20], the low acceleration level available to LIC offers significant challenges for the design of orbits and transfers that are mitigated in this investigation by utilizing the modified orbit chaining approach described in the previous section.

To illustrate the performance of the design framework, consider a low-thrust transfer for the 14 kg LIC spacecraft —with a maximum acceleration level of $8 \times 10^{-5} m/s^2$— from the assumed L_2 Southern (S) Near Rectilinear Halo Orbit (NRHO) primary science mission orbit with energy $JC = 3.0553$ to a circular planar retrograde Low lunar Orbit (LLO) with energy $JC = 3.2541$. This target arrival orbit is a member of the family of lunar Distant Retrograde Orbits The departure and arrival orbits are depicted in Figure 8 and exist within the context of the CR3BP.

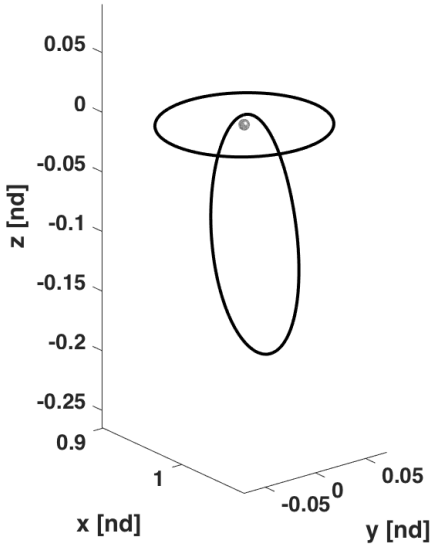

Figure 8. Departure and Arrival Orbits within the Context of the CR3BP.

The modified adaptive orbit chaining methodology suggests that, instead of approaching the problem as a direct transfer from departure to destination, a family of arrival orbits is populated —with the original circular LLO as the last member of the family— such that, the transfer design problem is divided into as many subproblems as the number of orbit members in the newly created family of arrival orbits. An illustration of the family of arrival orbits is presented in Figure 9, where each colored orbit member represents a continued member of the family from the original destination circular LLO.

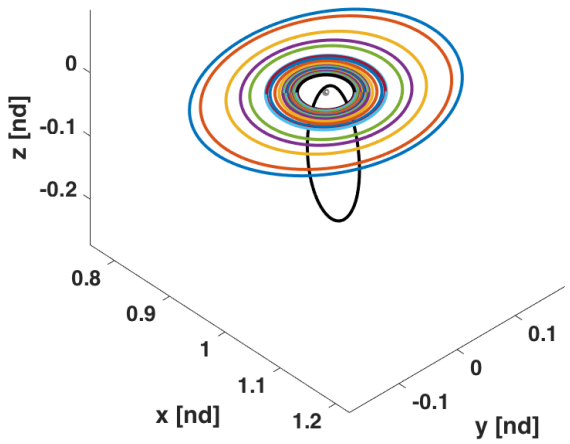

Figure 9. Family of Arrival Orbits within the Context of the CR3BP. The Original Target Destination Orbit is Represented by the Smaller Orbit in Black

The first subproblem of the modified orbit chaining methodology consist of constructing a low-thrust transfer from the L_2 S NRHO to the outer most blue orbit in Figure 9. The framework leverages an energy based parametrization of the space to identify informed candidates as intermediate arcs —i.e., traditional orbit chaining scheme— for connecting the departure and arrival orbits. The initial guess is then generated by a sliding adaptive algorithm in the CR3BP-LT model and it is plotted in Figure 10(a), while the converged solution, in the same force model, appears in Figure 10(b); Blue and red arcs correspond to coast and thrust segments, respectively.

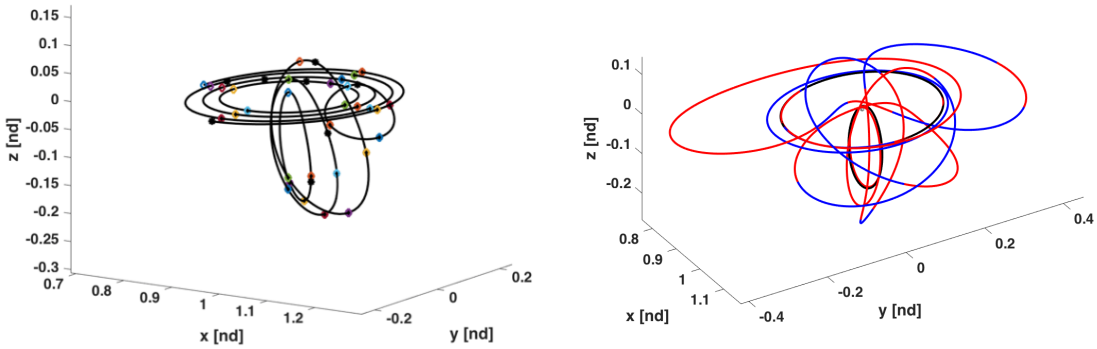

(a) First SubProblem - Initial Guess

(b) First SubProblem - Converged Transfer

Figure 10. Mass Optimal LT Transfer from a L_2 S NRHO to the First Member of the Family of Destination Orbits in the CR3BP-LT Model

As observed from Figure 10, the spacecraft travels from departure to destination without ever departing the vicinity of the Moon; instead, it slides through various members of families of periodic orbits that exist in the lunar vicinity to accomplished the required transfer. The energy —within the context of the CR3BP— and the thrust acceleration evolution for the converged solution are represented in Figure 11(a), while the time history of the thrust orientation angles are depicted in Figure 11(b).

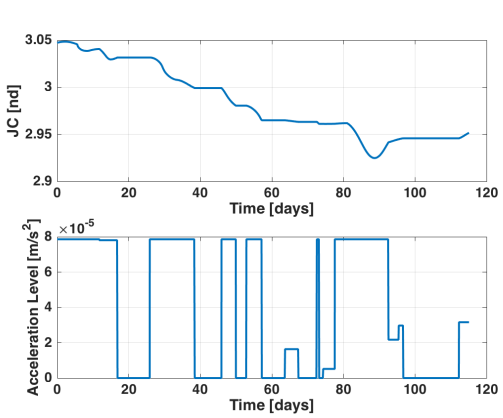

(a) First SubProblem - Energy and Thrust Acceleration Evolution

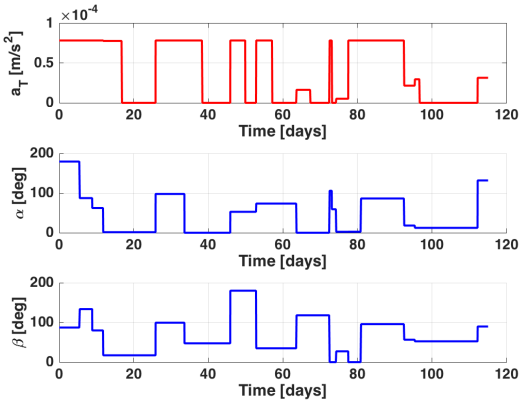

(b) First SubProblem - Thrust Orientation Evolution

Figure 11. Performance for a Mass Optimal LT Transfer from a L_2 S NRHO to the First Member of the Family of Destination Orbits in the CR3BP-LT Model

For the first subproblem in the CR3BP-LT model, the spacecraft requires 118.0373 days from the time it departs the original orbit (represented in Figure 10 as the first thrusting arc) until arrival on the destination orbit (i.e., the last thrusting arc). In terms of propellant consumption, the transfer path requires about 0.2199kg (1.57%) of the 14kg initial mass, which corresponds to an equivalent ΔV of $388.1579m/s$. This performance is quantified in terms of the trade-off between transfer time, propellant consumption, and the spacecraft's ability to remain within the region of interest in space. Furthermore, transitioning these results to a higher fidelity ephemeris model produces the transfer trajectories illustrated in Figures 12(a) and (b) for a Earth-centered inertial frame and a Moon-centered inertial frame respectively. In the ephemeris model, the ΔV decreases to $369.7857m/s$. However, recall that in the higher-fidelity model, the performance is dependent upon the epoch.

By employing a continuation method on the arrival orbit, the solution to the first subproblem is utilized as the initial guess to construct a low-thrust transfer for the second subproblem —i.e., a transfer from the departure L_2 S NRHO to the second to last most outer member of the family of arrivals orbits shown in Figure 9. The initial guess for the second subproblem is the converged transfer illustrated in Figure 10. The process is continued for each arrival orbit in the family of destination orbits, one of which yields the trajectory depicted in Figure 13(b). As it is expected, the transfer geometry resembles that of the initial guess, represented in Figure 13(a). Furthermore, in this particular scenario, the spacecraft requires 135.7805 days from the time it departs the original orbit (represented in Figure 13 as the first thrusting arc) until arrival on the destination orbit (i.e., the last thrusting arc). In terms of propellant consumption, the transfer path requires about 0.2199kg (1.57%) of the 14kg initial mass, which corresponds to an equivalent ΔV of $304.7811m/s$. This performance is represented Figure 14 in terms of the energy and the thrust parameters evolution

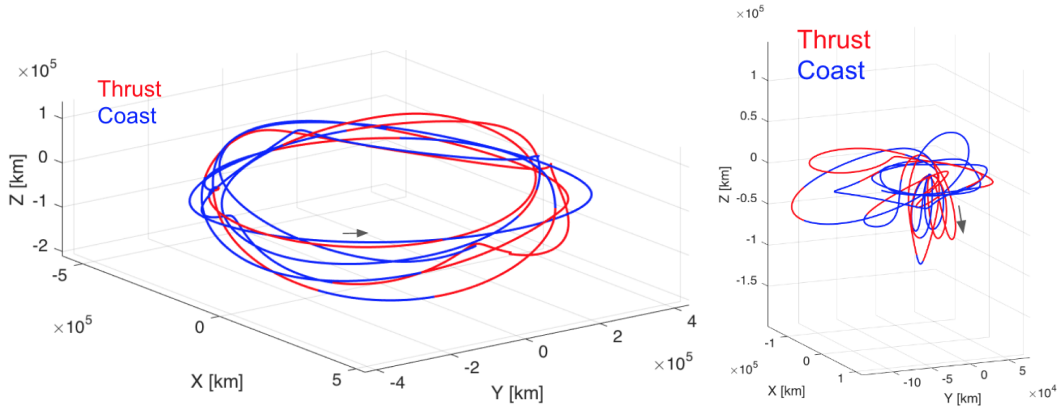

(a) First SubProblem - Earth-centered Inertial View

(b) First SubProblem - Moon-centered Inertial View

Figure 12. Mass Optimal LT Transfer from a L_2 S NRHO to the First Member of the Family of Destination Orbits in the Ephemeris Model

in time. Transitioning these results into a higher fidelity ephemeris model yields the trajectories in Figure 15, for which the ΔV consumption for the particular epoch examined corresponds to $334.6225 m/s$.

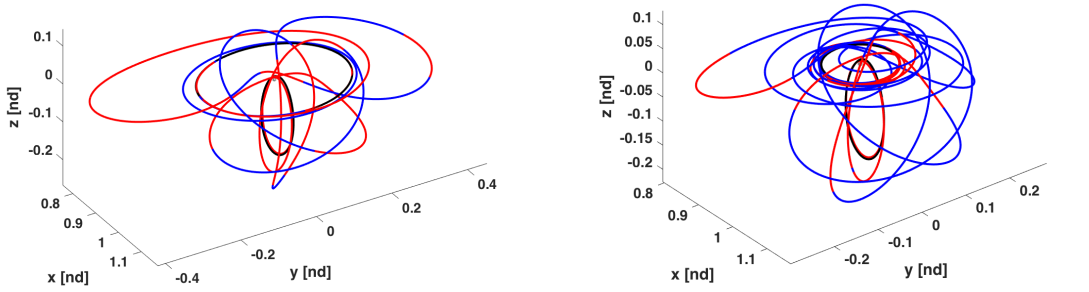

(a) Intermediate SubProblem - Initial Guess

(b) Intermediate SubProblem - Converged Transfer

Figure 13. Mass Optimal LT Transfer from a L_2 S NRHO to an Intermediate Member of the Family of Destination Orbits in the CR3BP-LT Model

Overall, this trajectory design problem is divided into 21 subproblems (since the family of arrival orbits is comprised of 21 members), each of which utilizes the converged mass optimal solution from the previous subproblem, to generate a fully converged solution for the subproblem at hand. Moreover, note that, with this modified orbit chaining framework, the traditional orbit chaining framework combined with the energy-informed adaptive sliding algorithm is employed only once to construct the solution for the first subproblem, while the remaining subproblems are obtained via a continuation scheme.

The solution to the last subproblem, that corresponds to the solution to the original low-thrust

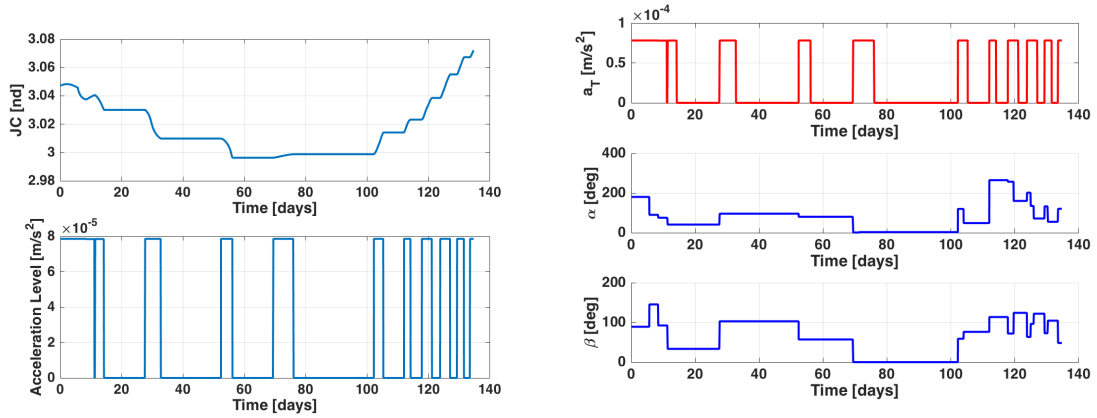

(a) Intermediate SubProblem - Energy and Thrust Acceleration Evolution

(b) Intermediate SubProblem - Thrust Orientation Evolution

Figure 14. Performance for a Mass Optimal LT Transfer from a L_2 S NRHO to an Intermediate Member of the Family of Destination Orbits in the CR3BP-LT Model

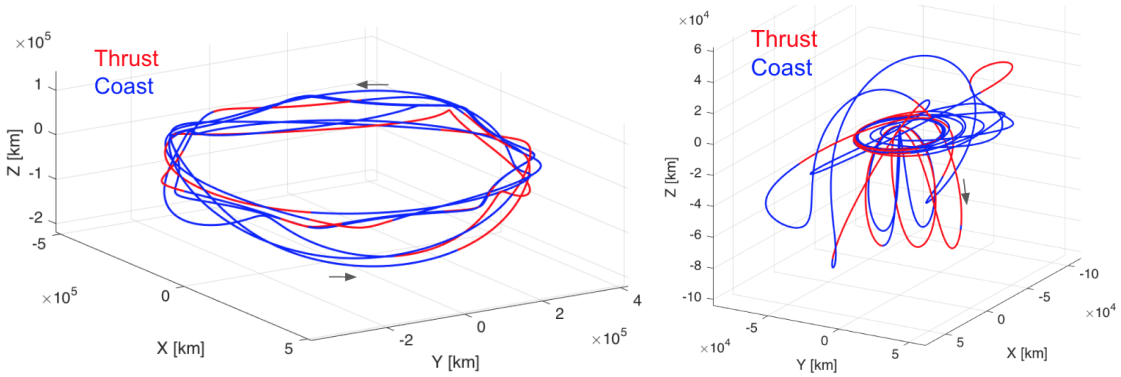

(a) Intermediate SubProblem - Earth-centered Inertial View

(b) Intermediate SubProblem - Moon-centered Inertial View

Figure 15. Mass Optimal LT Transfer from a L_2 S NRHO to an Intermediate Member of the Family of Destination Orbits in the Ephemeris Model

transfer sought in this application, is illustrated in Figure 16, where it is seen that the geometry of the transfer once more resembles that of the initial guess utilized for its construction —i.e., as expected, the geometry of the trajectories in Figures 10 and 16 are consistent. Blue arcs correspond to segments where the engine is coasting, while the red portions of the trajectory correspond to the times at which the spacecraft is thrusting. Evidently, the spacecraft takes a longer duration of time to reach its final destination orbit, and the thrust arcs grow larger and larger as the altitude of the destination orbit grows closer to the Moon. In fact, the geometry of the trajectory resembles spiral arcs, that are known to be native to low-thrust transfers in the vicinity of a primary body.

The performance in terms of the time evolution of the energy and the thrust parameters are shown in Figure 17. In this case, the spacecraft requires 156.3855 days to transfer from the original L_2 S NRHO to the final target circular LLO, and its propellant consumption corresponds to 0.3371 kg of the initial 14 kg mass. Furthermore, if the propellant consumption is transformed into equivalent

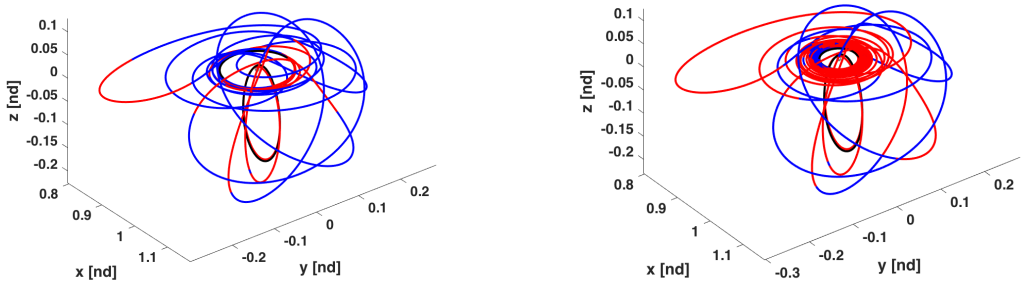

(a) Last SubProblem - Initial Guess

(b) Last SubProblem - Converged Transfer

Figure 16. Mass Optimal LT Transfer from a L_2 S NRHO to a Circular LLO in the CR3BP-LT Model

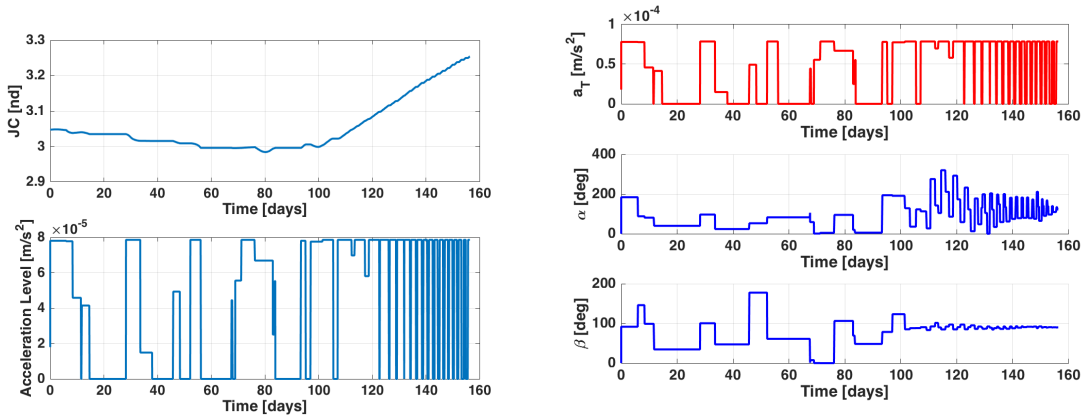

(a) Last SubProblem - Energy and Thrust Acceleration Evolution

(b) Last SubProblem - Thrust Orientation Evolution

Figure 17. Performance for a Mass Optimal LT Transfer from a L_2 S NRHO to a Circular LLO in the CR3BP-LT Model

ΔV, it corresponds to a total of $597.5081 m/s$.

CONCLUDING REMARKS

Low-thrust spacecraft trajectory design in the cislunar region is highly driven by the dynamical regime utilized to describe the equations of motion. To accurately represent this dynamical environment, different levels of fidelity —the two-body problem, the circular restricted three-body problem system and the higher-fidelity ephemeris model—, are considered in this investigation, and presented for applications of vehicles traveling between libration point orbits in the Earth-Moon system. A new method for constructing initial guesses, for transfers between libration point orbits in the Earth-Moon CR3BP-LT system, has been explored, via exploitation of the energy parametrization of the periodic orbit families.

A natural parameter continuation method is successfully introduced into the implementation of a generalized modified orbit chaining technique, that leverages an energy-informed adaptive sliding algorithm to navigate the cislunar space in the creation of informed initial guesses, and delivers optimal trajectories for low-thrust spacecraft moving in the vicinity of the Moon, that are easily transition from lower fidelity force models into a higher fidelity model that includes the gravitational attraction of the Sun, the Earth and the Moon. The type of low-thrust engine examined in this investigation is consistent with the electric propulsion technology, whose efficiency and capabilities are continuously evolving. This feature signifies for the low-thrust trajectory design framework to be flexible enough such that it does not depend on the type of vehicle utilized, nor on the dynamical model employed to construct the initial estimate for the low-thrust transfer.

ACKNOWLEDGMENTS

The authors would like to thank the members of the Multibody Dynamics Research Group at Purdue University, as well as the Visualization lab for use of computing resources. Portions of this work were supported by the Purdue University Minority Engineering Program. The authors also appreciate partial support from NASA Grant 80NSSC20K1117.

REFERENCES

[1] Hambleton, K. "Deep Space Gateway to Open Opportunities for Distant Destinations." NASA, (March 28, 2017) *https://www. nasa. gov/feature/deep-space-gateway-to-open-opportunities-for-distant-destinations*. 24 August 2018

[2] Folta, D.C., Bosanac, N., Cox, A. and Howell, K.C. "The Lunar IceCube Mission Design: Construction of Feasible Transfer Trajectories With a Constrained Departure." *AAS/AIAA Space Flight Mechanics Meeting*, February 2016, AAS 16-285.

[3] R. Pritchett, "Strategies for Low-Thrust Transfer Design Based on Direct Collocation Techniques," Ph.D. Thesis, School of Aeronautics and Astronautics, Purdue University, 2020

[4] M. D. Rayman, "The Successful Conclusion of the Deep Space 1 Mission: Important Results Without a Flashy Title," 53rd International Astronautical Congress. Houston, TX, pp. 1?13, 2002

[5] C. Russell and C. Raymond, The Dawn Mission to Minor Planets 4 Vesta and 1 Ceres. New York: Springer-Verlag, 2012

[6] J. Kawaguchi, A. Fujiwara, and T. Uesugi, "Hayabusa-1 its Technology and Science Accomplishment Summary and Hayabusa-2," Acta Astronautica, vol. 62, pp. 639?647, 2008

[7] M. W. Lo and J. S. Parker, "Chaining Simple Periodic Three Body Orbits," AAS/AIAA Astrodynamics Specialist Conference. Lake Tahoe, California, 2005.

[8] B. Prado Pino, K. C. Howell, and D. C. Folta, "An Energy-Informed Adaptive Algorithm for Low-Thrust Spacecraft Cislunar Trajectory Design," AAS/AIAA Astrodynamics Spe- cialist Conference, 2020

[9] B. Prado Pino, K. C. Howell, D. C. Folta, and R. E. Pritchett, "Extended Mission Options for the Lunar IceCube Low-Thrust Spacecraft by Leveraging the Dynamical Environment,? 71st International Astronautical Congress, 2020.

[10] Pritchett, R., Zimovan, E. and Howell, K.C. "Impulsive and Low-Thrust Transfer Design between Stable and Nearly Stable Periodic Orbits in the Restricted Problem." *18th AIAA SciTech Forum*, Kissimmee, Florida, January 2018.

[11] McGuire, M.L., Burke, L.M., McCarty, S.L., Hack, K.J., Whitley, R.J., Davis, D.C. and Ocampo, C. "Low Thrust Cis-Lunar Transfers Using a 40 KW-Class Solar Electric Propulsion Spacecraft." *AAS/AIAA Space Flight Mechanics Meeting*, February 2017, AAS 17-583.

[12] Lantoine, G. "Efficient NRHO to DRO Transfers in Cislunar Space." In *AAS/AIAA Astrodynamics Specialist Conference*, August 2017, pp. 1-18.

[13] F. Diacu, "The Solution of the n-body Problem," The Mathematical Intelligencer, vol. 18, pp. 66?70, 3 1996

[14] Stuart, J., Ozimek, M. and Howell, K. "Optimal, Low-Thrust, Path-Constrained Transfers Between Libration Point Orbits Using Invariant Manifolds." In *AIAA/AAS Astrodynamics Specialist Conference*, 2010, p. 7831.

[15] N. Aeronautics and S. A. (NASA). (2019). “Nasa space science data coordinated archive”, [Online]. Available: https://nssdc.gsfc.nasa.gov/nmc/spacecraft/ display.action?id=1978-079A.

[16] T. A. Pavlak, “Trajectory design and orbit maintenance strategies in multi- body dynamical regimes”, Ph.D. Thesis, School of Aeronautics and Astronautics, Purdue University. West Lafayette, Indiana, May, 2013.

[17] J. S. Parker, K. E. Davis, and G. H. Born, “Chaining Periodic Three-Body Orbits in the Earth-Moon System,” Acta Astronautica, vol. 67, pp. 623?638, 2010.

[18] A. F. Haapala and K. C. Howell, “A framework for constructing transfers linking periodic libration point orbits in the spatial circular restricted three-body problem,” International Journal of Bifurcation and Chaos, vol. 26, 2016.

[19] N. Bosanac, A. D. Cox, K. C. Howell, and D. C. Folta, “Trajectory Design for a Cislunar CubeSat Leveraging Dynamical Dystems Techniques: The Lunar IceCube Mission,? Acta Astronautica, vol. 144, pp. 283?296, 2018.

[20] Williams, J., Lee, D.E., Whitley, R.J., Bokelmann, K.A., Davis, D.C. and Berry, C.F. “Targeting Cislunar Near Rectilinear Halo Orbits for Human Space Exploration.” *AAS/AIAA Spaceflight Mechanics Meeting*, February, 2017.